Korean J. Chem. Eng., 33(9), 2602-2609 (2016)
DOI: 10.1007/s11814-016-0128-0

pISSN: 0256-1115
eISSN: 1975-7220

Electrochemical removal of the insecticide imidacloprid from water on a boron-doped diamond and Ta/PbO_2 anodes using anodic oxidation process

Mabrouk Ben Brahim†, Hafedh Belhadj Ammar, Ridha Abdelhédi, and Youssef Samet

Electrochemistry and Environmental Laboratory, Department of Materials Engineering, National Engineering School of Sfax, University of Sfax, B. P. 1173, 3038, Sfax, Tunisia
(*Received 2 September 2015 • accepted 5 May 2016*)

Abstract−The removal of pesticides from water is a major environmental concern. This study investigates the electrochemical removal of the insecticide imidacloprid (IMD) from aqueous solutions on a boron-doped diamond (BDD) and Ta/PbO_2 anodes under galvanostatic electrolysis. The influence of operating parameters, such as applied current density (50-100 mA cm^{-2}), initial chemical oxygen demand COD (0) (281-953 mg L^{-1}), temperature (25-65 °C) and pH (3.0-10.0) on COD and instantaneous current efficiency (ICE), was studied using the BDD electrode. The degradation efficiency of IMD increased by increasing current density and temperature, but noticeably decreased by the increase of initial pH value and initial concentration of IMD. The COD decay follows a pseudo-first-order kinetic, and the process was under mass transport control. COD removal reaches 90% when using an apparent current density of 100 mA cm^{-2}, initial COD of 953 mg L^{-1}, pH of 3.0 and at 25 °C after 4.5 h electrolysis time. Compared with Ta/PbO_2, BDD anode has shown better performance and rapidity in the COD removal using the same electrolysis device.

Keywords: Pesticides, Imidacloprid, Electrochemical Degradation, Electrolysis, Boron-doped Diamond, Hydroxyl Radicals

INTRODUCTION

Pesticides are the most abundant environmental pollutants found in soil, water, atmosphere and agricultural products. Organochlorine compounds comprise a diverse group of chemicals that are extensively used as insecticides in modern agriculture. Among these, imidacloprid (IMD) is one the most commonly used pesticides for crop protection worldwide, due to its low soil persistence and high insecticidal activity at very low application rate [1]. It is used worldwide to control a number of agricultural insects, such as aphids, whiteflies, leafhoppers, termites [2]. The intensive use of IMD in agriculture and improper storage are the main sources of contamination. A number of researchers have reported residues of IMD in different agriculture crops substrate [3-5]. The major degradation product of IMD in water and soil was proposed (Fig. 1) [6]. However, the presence of this pesticide residue is extremely hazardous to human health and other living organisms. For this reason, it is highly important to develop technologies for the removal of these insecticides in order to decrease their impact on the environment. Various methods have been used for the removal of IMD, such as photocatalytic degradation, using TiO_2 as catalyst [7-10], photo-Fenton [11,12], biological oxidation [13,14], chemical oxidation with ozone [15,16] and adsorption [17,18]. However, these processes are quite expensive and involve several operational problems. Thus, there has been an increasing interest in the use of new methods, namely electrochemical oxidation.

Electrochemical oxidation has become one of the most promising techniques for the treatment of wastewaters, which is environmentally compatible with the cleanest reactant, electron, easy to control and without secondary pollution [19,20]. Hitherto, various types of electrodes materials have been examined for IMD removal, including TiO_2/Ti [9-10], Ti/TiO_2/Rh_2O_3 [21], graphite electrode [22], Ti/SnO_2-Sb_2O_3 [23]. The electrochemical degradation of insecticide IMD from water by anodic oxidation and electro-Fenton processes was studied using BDD anode [24]. The results showed that both anodic oxidation and electro-Fenton process exhibited high mineralization efficiency, reaching 91 and 94% of total organic carbon (TOC) removal at 2 h, respectively.

Recently, Iglesias et al. [25] studied the removal of IMD by a heterogeneous electro-Fenton system with iron alginate gel beads (EF-FeAB). The effects of the initial pH and initial concentration of alginate beads (FeAB) on the IMD removal rate were studied. The removal efficiency was maintained with an increase in Fe dosage and decreased with an increase in the initial pH. The optimum dose IMD removal was observed within 120 min at an initial pH of 2. Wang et al. [26] studied the electrochemical treatment of IMD solutions by electrosorption enhanced electro-Fenton (ES-EF) process with mixed-valence iron oxide grown on bulk activated carbon aerogel (FeO_x/ACA) as cathode. The results revealed that the TOC removal WAS 93% after 150 min of treatment. Zhao et al. [27] degraded the pesticide IMD by employing an Fe_3O_4/Fe_2O_3/activated carbon aerogel cathode within a wide range of pH, leading to 90% removal after 30 min of treatment.

The development of a novel electrochemical technique using BDD electrode can provide a priceless service in the monitoring of the compounds that are important in terms of human health defense, environment and food chemistry. BDD electrodes have been excellently used as an alternative to other conventional anodes, for in-

†To whom correspondence should be addressed.
E-mail: benbrahim.mabrouk@yahoo.com

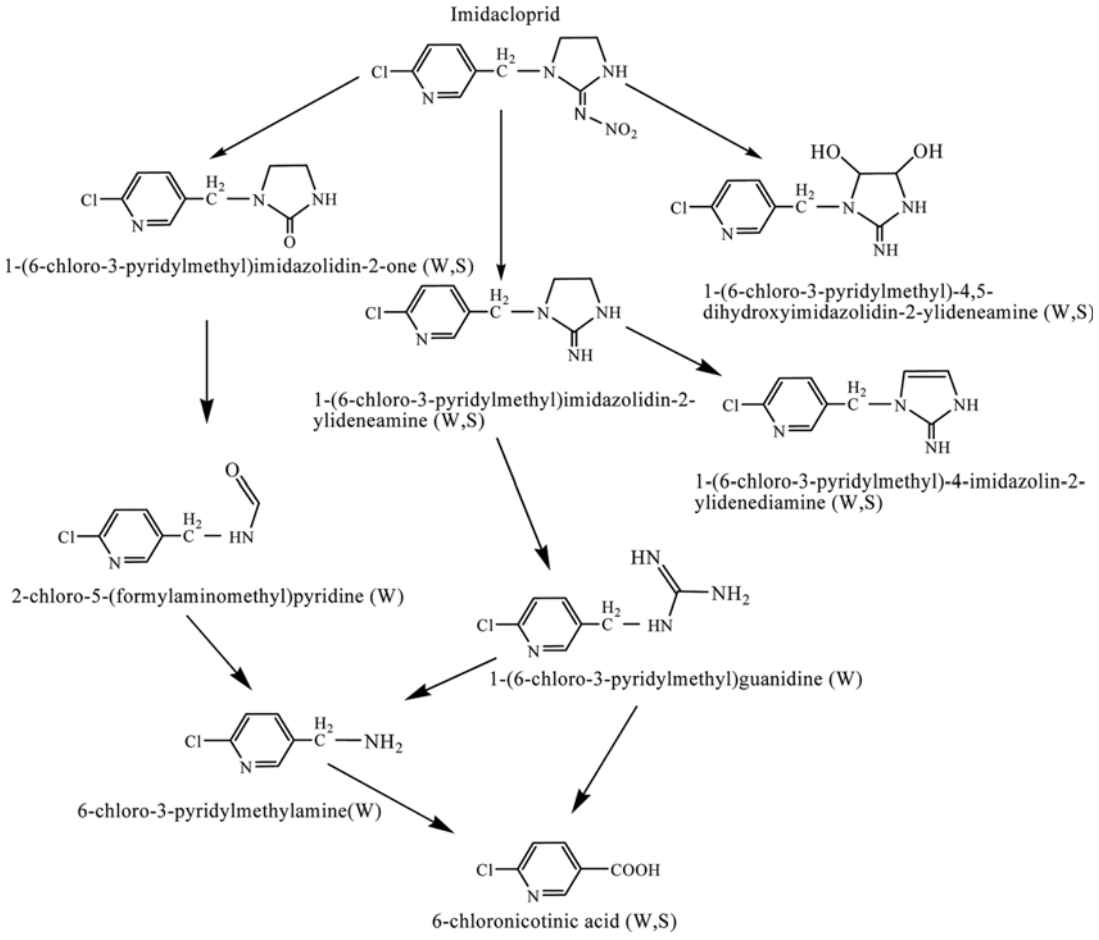

Fig. 1. Metabolic pathway for Imidacloprid. Metabolite or degraded found in: (S) soil and (W) water [6].

stance: PbO_2, doped SnO_2, IrO_2 and Pt, then producing larger amount of $HO^{\bullet}$. It has several important characteristics, including an inert surface with low adsorption proprieties, remarkable corrosion stability, even in strong acidic media, an extremely wide potential window in aqueous solutions (up to 3.5 V) and high reproducibility of electrochemical responses [28-30].

However, many studies on electrochemical treatment of organic compounds at BDD anode [31-35] indicate that the BDD anode has displayed noticeable oxidation ability for treating wastewaters. PbO_2 anode directly electrodeposited on a tantalum substrate has also been used because of the electrochemical and chemical stability of this metal oxide as anode [36]. From the voltage-pH diagram, tantalum passivates on contact with an aqueous solution by the formation of the non-conducting oxides Ta_2O_5 [37].

The present work represents a focus on the study of the electrochemical degradation of the IMD on the BDD and the Ta/PbO_2 anodes.

EXPERIMENTAL

1. Chemicals

In this work, all solutions were prepared in the laboratory. These solutions contain quantities of IMD taken from an emulsifiable concentrate (Confidor 200 SL from Bayer CropScience) containing 200 g L^{-1} IMD. All solutions were freshly prepared with double-distilled water. Sodium hydroxide (NaOH) and sulfuric acid (H_2SO_4) of analytic grade were employed as conductive electrolytes and for pH adjustment. Standard solutions of potassium dichromate ($K_2Cr_2O_7$), sulfuric acid (H_2SO_4) reagent with silver sulfate (Ag_2SO_4) were prepared to measure the COD.

2. Boron-doped Diamond Si/BDD Electrode

The boron-doped diamond electrode was provided by CSEM (Center Swiss for Electronics and Microtechnology, Neuchâtel, Switzerland). It was synthesized by the hot filament chemical vapor deposition technique (HF-CVD) [38] on single-crystal p-type Si (100) wafers (1-3 mΩ cm, Siltronix). The doping level of boron in the diamond layer, expressed as B/C ratio, was about 3,500 ppm. The resulting diamond film thickness was about 1 μm with a resistivity of 10-30 mΩ cm. The electrode area was 6 cm^2. Prior to use in galvanostatic electrolysis assays, the electrode was polarized during 30 min with a 1 M H_2SO_4 solution at 50 mA cm^{-2} to remove any kind of impurity from its surface.

3. Preparation of the Ta/PbO_2 Electrode

3-1. Tantalum Surface Treatment

Pretreatments of the tantalum substrate (rectangular tantalum plates 6 cm×1 cm×0.1 cm) were carried out before anodization to ensure good adhesive lead dioxide film. Tantalum was first roughened to increase the adhesion of PbO_2 deposit via subjecting its

surface to mechanical abrasion using silica grains with an average diameter of 0.3 mm projected under 5 bar pressure. Subsequently, it was cleaned to remove sand particles or any other particles lodged in the metal surface. This was conducted by degreasing with acetone, due to its ease of application and its great penetrating power, and then ultrasonically rinsed in ultrapure water during 10 min. Uniform and good adhesive deposit necessitates a smooth surface with no oxides (formed spontaneously on contact with oxygen in the air) or scales. To ensure this, the tantalum substrate was soaked for 30 s in hydrofluoric acid (40% weight) at room temperature and then abundantly rinsed with ultrapure water.

3-2. Electrochemical Deposition of PbO_2

The lead dioxide was deposited galvanostatically on the pretreated tantalum substrate by electrochemical anodization of an aqueous $Pb(NO_3)_2$ solution (1 M) placed in a tow-compartment Pyrex glass cell (V=150 cm^3) thermoregulated at 65 °C. The electrodeposition of PbO_2 film was carried out at an apparent current density of 10 mA cm^{-2} for 0.5 hours, then at 20 mA cm^{-2} for the same period and finally at 50 mA cm^{-2} for one hour. The average mass of PbO_2 was 0.21 g cm^{-2}. The deposit obtained was a grey porous material with strong adherence.

4. Electrolysis

Galvanostatic electrolysis of IMD aqueous solutions (150 cm^3) was carried out in a two-compartment thermostatic cell (Fig. 2). The cathode was a cylindrical polycrystalline platinum grid (Φ=4 cm, L=6 cm) placed in a porous ceramic cylinder (Norton, RA 84) containing 2 g L^{-1} sodium sulfate solution. The anodes were BDD (6 cm^2) or Ta/PbO_2 plate (6 cm^2) symmetrically around the cathode. IMD solutions were electrolyzed in galvanostatic mode by using a DC power supply (model ABTP 530 Française d'Instrumentation, France). The range of applied current density was 50 to 100 mA cm^{-2}. The pH of solution was adjusted, before and over the course of the electrolysis, by adding either concentrated sulfuric acid or sodium hydroxide solutions.

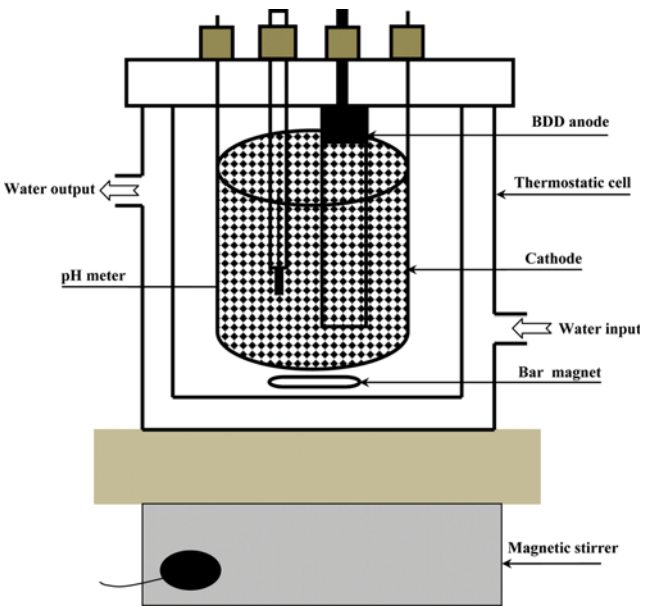

Fig. 2. Electrolytic cell.

5. Analysis

5-1. Chemical Oxygen Demand COD

Chemical oxygen demand COD is a measure of the oxygen equivalent to organic matter content of a sample that is susceptible to the oxidation by strong chemical oxidant.

The COD measurement during the processing permitted the evaluation of the kinetic of organic matter decay and the instantaneous current efficiency (ICE). COD was determined by the dichromate method [39]. The appropriate amount of sample was introduced into prepared digestion solution containing potassium dichromate, sulfuric acid and mercury (II) sulfate. Afterwards, the mixture was incubated for 2 hours at 150 °C in a WTW CR 2200 thermoreactor (Germany) for COD and thermal digestion. COD concentration was measured colorimetrically using DR/2010 spectrophotometer (Hach Company, USA). The absorbance measurements involved using a UV-visible spectrophotometer (Shimadzu 1650 PC). The instantaneous current efficiency (ICE) can be defined as the part of the current directly used for the oxidation of the organic compounds. It can be performed from the decrease of COD by means of the following relation [40] (Eq. (1)).

$$ICE = \frac{COD(t) - COD(t+\Delta t)}{8It} FV \quad (1)$$

where, F is the Faraday constant (96,487 C/mol), V the volume of the solution (L), COD (t) and COD (t+Δt) are the chemical oxygen demands at times t and t+Δt (in g O_2 L^{-1}), respectively, and I is the current (A).

The specific energy consumption (kWh/m^3) was calculated by Eq. (2):

$$Ec = \frac{U_{cell} It}{3600\ V} \quad (2)$$

where U_{cell} is the average cell voltage (V), I is the current (A), t is electrolysis time (s) and V is the volume (L).

RESULTS AND DISCUSSION

1. Effect of Different Operating Factors on Degradation of IMD using BDD Anode

1-1. Effect of Current Density

Applied current density is an important factor affecting the electrolysis kinetics and process economics. The effect of applied current on the electrochemical process was demonstrated in several studies [41-43]. The influence of the current density on the COD removal during the electrochemical oxidation of IMD at the BDD anode is shown in Fig. 3. As can be seen, the rate of IMD degradation was greatly dependent on the j_{app} and became faster with increasing current density. For example, after 270 min of electrolysis the COD percent removal increased from 53 to 90% when the current density increased from 50 to 100 mA cm^{-2}. This result can be explained by an increase of the amount of hydroxyl radicals with the increase of the applied current [44,45], according to Eq. (3).

$$BDD + H_2O \rightarrow BDD(HO^{\bullet}) + H^+ \quad (3)$$

The decay of COD concentration exhibits an exponential behavior with all the applied current, indicating first-order reaction kinetics

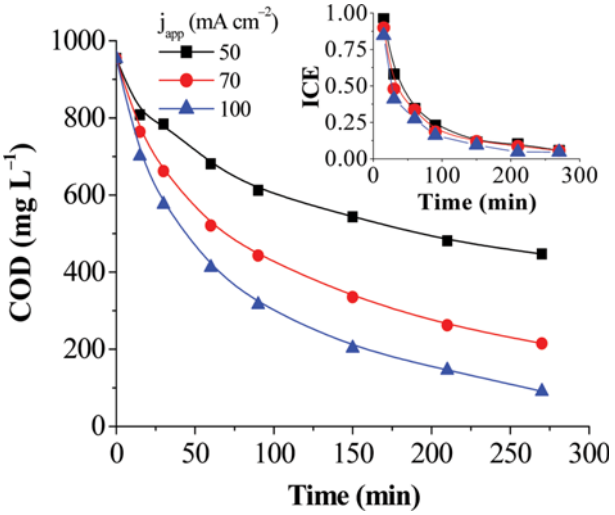

Fig. 3. Influence of the apparent applied current density on the trends of COD and ICE during electrolysis of IMD (COD(0)=953 mg L^{-1}) on the BDD anode. Electrolyte: Na_2SO_4 2 g L^{-1}; pH=3.0 and T=25 °C.

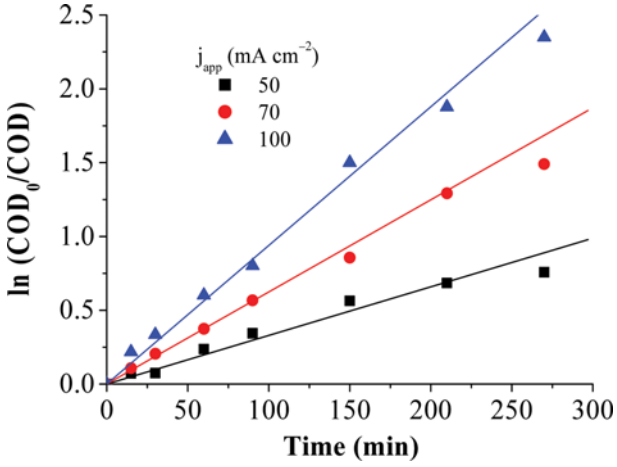

Fig. 4. Linear regression of the COD with time during electrolysis of IMD (COD(0)=953 mg L^{-1}) on the BDD anode for different current densities. Electrolyte: Na_2SO_4 2 g L^{-1}; pH=3.0 and T=25 °C.

for the oxidation reaction. Working in galvanostatic condition, the concentration of hydroxyl radical can be approximated in a steady state and, therefore, the oxidation rate expression can be written by Eq. (4):

$$r=\frac{-dCOD}{dt}=k[HO^{\bullet}]^{\alpha}COD(t)=k_{app}COD(t)=\frac{Ak_m}{V}COD(t) \quad (4)$$

where, α is the reaction order related to the hydroxyl radicals, k is the real rate constant, k_{app} is the global apparent rate constant for COD removal, k_m is overall mass transfer coefficient, A is the electrode area (m^2) and V is the volume of the treated solution (m^3).

We assumed that hydroxyl radical's concentration was constant during the electrolysis; therefore,

$$k[HO^{\bullet}]^{\alpha}=k_{app} \quad (5)$$

The integration of the previous equation is subject to the initial condition COD(t)=COD(0) at t=0 leads to the Eq. (6):

$$COD(t)=COD(0)\exp\left(-\frac{Ak_m}{V}t\right) \quad (6)$$

where k_m can be calculated from the slope value of the plot of ln[COD(0)/COD(t)] versus t (Fig. 4). The straight lines obtained in these plots were in agreement with a pseudo-first-order COD removal.

As shown in the inset of Fig. 3, the increased current density resulted in a decrease in current efficiency. The ICE can also be defined [46] by (Eq. (7)).

$$ICE=\frac{j_{lim}(t)}{j_{app}} \quad (7)$$

where, j_{lim} (t) is the limiting current density (A m^{-2}) and j_{app} is the applied current density (A m^{-2}).

j_{lim} (t) can be defined by Eq. (8), which is related to the electrochemical combustion of the IMD.

$$C_9H_{10}ClN_5O_2+31H_2O\rightarrow 9CO_2+66\,e^-+72H^++5NO_3^-+Cl^- \quad (8)$$

$$j_{lim}(t)=66\,Fk_mC(t) \quad (9)$$

where, 66 is the number of exchanged electrons in the IMD combustion and F is the faraday constant (96,487 C mol^{-1}).

The stoichiometry of IMD combustion indicates that 16.5 mol of O_2 are needed for the complete oxidation of IMD (Eq. (10)).

$$C_9H_{10}ClN_5O_2+16.5\,O_2\rightarrow 9CO_2+2H_2O+Cl^-+5NO_3^-+6H^+ \quad (10)$$

Thus, the IMD concentration C(t) in mol m^{-3}, during the electrolytic process, is related to the COD(t) (mol m^{-3}) by the following relation (Eq. (11)).

$$COD(t)=16.5\,C(t) \quad (11)$$

From Eqs. (9) and (11) the limiting current density at a given time t can be written as a function of COD (t) (Eq. (12)).

$$j_{lim}(t)=\frac{66}{16.5}Fk_mCOD(t)=4Fk_mCOD(t) \quad (12)$$

At the beginning of the electrolytic process (t=0), the initial limiting current density is given by the following equation:

$$j_{lim}(0)=4Fk_mCOD(0) \quad (13)$$

Two kinetics regimes can be defined depending on the value of the applied current density j_{app}:

- If j_{app} is lower than $j_{lim}(0)$, the electrolysis is under charge transfer control; the instantaneous current efficiency is then 100%.
- If j_{app} is higher than $j_{lim}(0)$, the electrolysis is under mass-transport control; secondary reactions (such as oxygen evolution) occur.

The data taken from Table 1 indicate that j_{app} values are higher than $j_{lim}(0)$ values and the current efficiency is below 100% (inset of Fig. 3), revealing that the degradation process of IMD was controlled by mass transfer in the tested current density range. Moreover, increasing the applied current density increases the diffusion flux of organic matter towards the anode surface. This results in a decrease in the diffusion layer thickness, and consequently an in-

Table 1. Effect of the applied current density (j_{app}) on the values of mass transfer coefficient (k_m) and initial limiting current density ($j_{lim}(0)$)

j_{app} (mA cm^{-2})	$k_m \times 10^5$ (m s^{-1})	$j_{lim}(0)$ (mA cm^{-2})
50	1.37	19.72
70	2.60	37.43
100	3.75	53.98

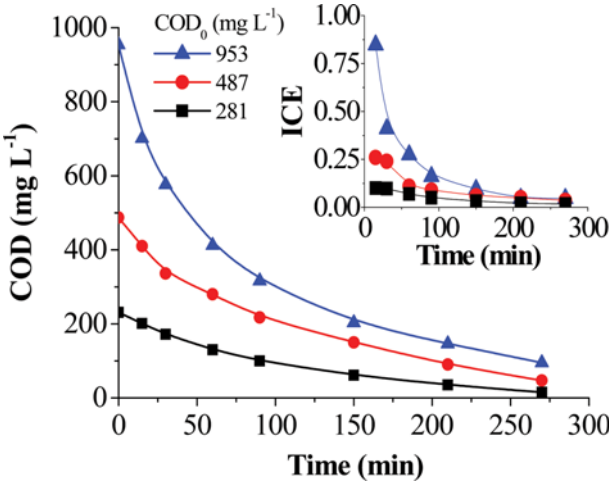

Fig. 5. Influence of the initial COD on the trends of COD and ICE during electrolysis of IMD on the BDD anode. Electrolyte: Na_2SO_4 2 g L^{-1}; j_{app}=100 mA cm^{-2}; pH=3.0 and T=25 °C.

crease of k_m values (k_m increased from 1.37×10^{-5} to 3.75×10^{-5} m s^{-1} when j_{app} increased from 50 to 100 mA cm^{-2}).

1-2. Effect of the Initial Concentration of IMD

The initial concentration of pesticide is always an important parameter in wastewater agricole treatment. Fig. 5 shows the trend of COD removal with time during electrolysis of IMD at different initial concentrations (COD(0): 281, 487, and 953 mg·L^{-1}) using an apparent current density of 100 mA·cm^{-2}, pH 3.0 and temperature 25 °C. The results indicate that COD percent removal decreased with an increase in initial COD. For example, after 270 min of electrolysis, COD percent removal decreased from 98 to 90% when initial COD increased from 281 to 953 mg·L^{-1}.

The inset of Fig. 5 displays the effect of instantaneous current efficiency (ICE) on the destruction of IMD solution, carried out at 100 mA cm^{-2}. As can be seen, the ICE decreases exponentially with time; this decay can be explained by the reaction of HO$^{\bullet}$ radicals with less organics reaching the anode by mass transfer.

1-3. Effect of Temperature

The electrolysis of the IMD solutions (COD(0)=953 mg L^{-1}) on the BDD anode at an applied current density of 100 mA cm^{-2} was carried out at different temperatures ranging from 25 to 65 °C. The increase in temperature had a positive effect on kinetic rate. The amount of organic matter decreased more quickly at 65 °C than at 25 °C (Fig. 6).

In fact, as shown in Fig. 7 and Table 2, the COD removal follows a pseudo-first-order kinetics and the k_{app} increased with temperature. After 150 min of electrolysis, the COD percent removal increased from 78 to 98% and k_{app} increased from 1.55×10^{-4} to 4.88×10^{-4} s^{-1} when the temperature increased from 25 to 65 °C. The in-

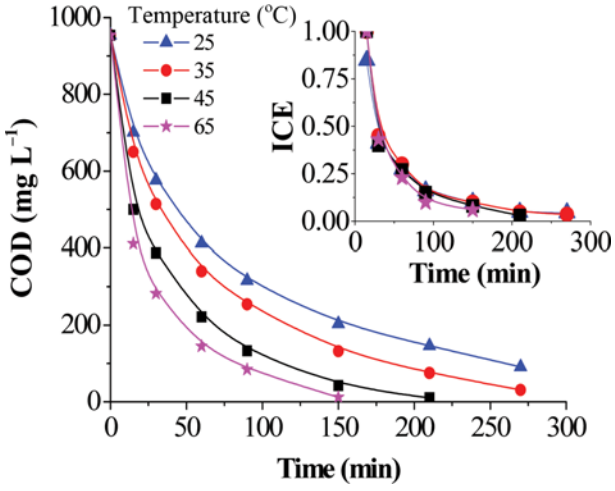

Fig. 6. Influence of the temperature on the trends of COD and ICE during electrolysis of the IMD (COD(0)=953 mg L^{-1}) on the BDD anode. Electrolyte: Na_2SO_4 2 g L^{-1}; j_{app}=100 mA cm^{-2} and pH=3.0.

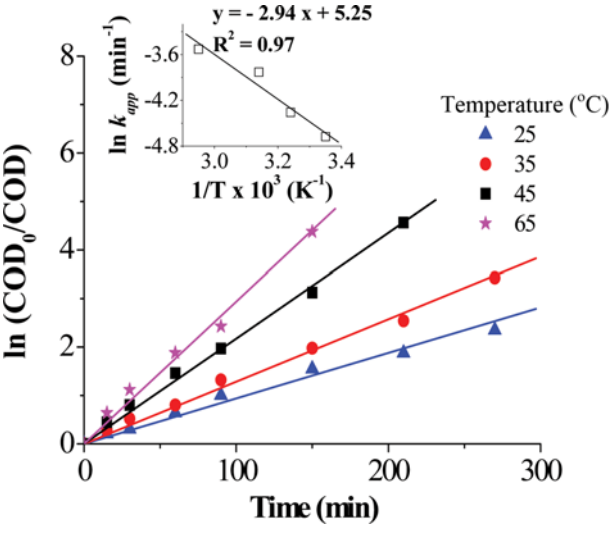

Fig. 7. Linear regression of COD removal with time during electrolysis of IMD (COD(0)=953 mg L^{-1}) on the BDD anode for different temperatures. Inset: Arrhenius-type plot of the apparent first-order kinetic constants. Electrolyte: Na_2SO_4 2 g L^{-1}, j_{app}=100 mA cm^{-2} and pH=3.0.

Table 2. Apparent rate constants of IMD removal fitted by a first order model and COD removal using BDD anode under different temperatures

Temperature (°C)	$k_{app} \times 10^4$ (s^{-1})	COD removal (%)
25	1.55	78
35	2.13	86
45	3.61	95
65	4.88	98

crease of IMD removal efficiency with temperature could also be attributed to the electrogeneration of inorganic oxidizing agents (e.g., persulfate). Additionally, peroxodisulfates can be formed in solutions containing sulfates during the electrolysis using BDD electrode (Eq. (14)).

$$BDD(HO^{\bullet})+2\,SO_4^{2-} \Leftrightarrow BDD+S_2O_8^{2-}+2e^- \quad (14)$$

These reagents are known to be very powerful oxidants that can act as a mediator for the oxidation of organic pollutants. Moreover, the reaction rate between peroxodisulfate ions and organic compounds increases with temperature [47,48].

Furthermore, the decrease of the medium viscosity with the increase of the temperature raises the diffusion rate of organic matter to the anode surface. Consequently, it takes part in the increase of the COD removal rate [49].

The Arrhenius expression, which shows the relationship between the reaction temperature and k_{app}, is expressed as follows (Eq. (15)):

$$k_{app} = A\exp\left(-\frac{E_{app}}{RT}\right) \quad (15)$$

where, A is the pre-exponential factor, E_{app} is the apparent global activation energy (J mol^{-1}), R is the ideal gas constant (8.314 J mol^{-1} K^{-1}) and T is the reaction's absolute temperature (K). E_{app} and A in Arrhenius form Eq. (15) were determined as 24.44 kJ mol^{-1} and 183.09 min^{-1}, respectively. E_{app} for a diffusion-controlled homogeneous reaction is typically less than 40 kJ·mol^{-1} [50], the experimental result was considerably lower than this value; it is therefore likely that the limiting step of IMD oxidation is of a diffusional nature.

1-4. Effect of the Initial pH

The effect of solution initial pH on the electrooxidation of pesticide has been previously investigated [51-53]. Some authors reported that the oxidation process was more favorable in acidic media [51,53]; others indicated that the efficiency of the process was increased in alkaline media [52]. Accordingly, it can be concluded that the effect of pH strongly depends on the nature of the investigated pesticide. Therefore, the effect of pH on the degradation rate of IMD was studied at large pH range from acidic to basic. The solutions of IMD (COD(0)=953 mg L^{-1}) were electrolyzed at pH values of 3.0 to 10.0 (Fig. 8). As can be seen from this figure, the degradation of IMD in the acid medium is more efficient than the degradation in alkaline and neutral medium. After 270 min time of electrolysis, the COD percent removal increased from 50 to 82% when the pH decreased from 10.0 to 3.0. Hence, for the range of pH studied, a pH of 3.0 appeared to be the optimum value.

1-5. The Electrical Energy Consumption

An important factor in the electrochemical treatment of organic-containing effluents is the energy necessary to achieve the desired results. The efficiency of the electrolysis system depends on the energy consumption for the reduction of 1 kg COD of organic matter (in terms of COD), which is one of the most crucial factors in the economics of electrolysis. The electrical energy consumption (E_c) required to decompose the IMD dye's solution (COD(0) 953 mg L^{-1}) at different current densities was calculated by referring to Eq. (2) and shown in Fig. 9. It reveals that the energy consumption increases with the current density. This behavior can be explained by the increase of the side reaction of oxygen evolution, the formation of more refractory products, such as carboxylic acids which are hardly oxidable intermediates [54,55] and the decrease of organic content in the solution.

2. Comparison between BDD and Ta/PbO_2 Anode

Fig. 10 shows a comparison of the trend of COD removal and the current efficiency during the oxidation of IMD (COD(0)=953 mg L^{-1}) using Ta/PbO_2 and BDD anodes. Under the optimal conditions (j_{app}=100 mA cm^{-2} pH=3.0 and T=65 °C), the BDD anode provided an oxidation rate and current efficiency higher than the Ta/PbO_2 anode. After 2.5 hours of treatment, the percent removal of COD could reach 99% on BDD anode, whereas it was only 70% at the Ta/PbO_2 anode. Moreover, the ICE measured during the oxidation of IMD with the BDD anode was higher than the ICE

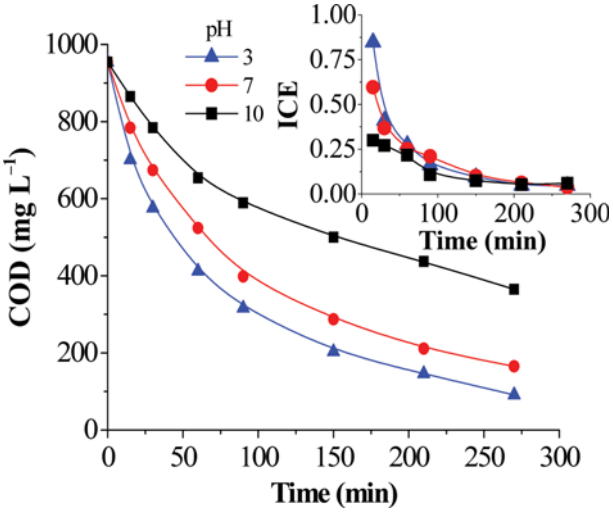

Fig. 8. Influence of pH on the trends of COD and ICE during electrolysis of IMD (COD(0)=953 mg L^{-1}) on the BDD anode. Electrolyte: Na_2SO_4 2 g L^{-1}; j_{app}=100 mA cm^{-2} and T=25 °C.

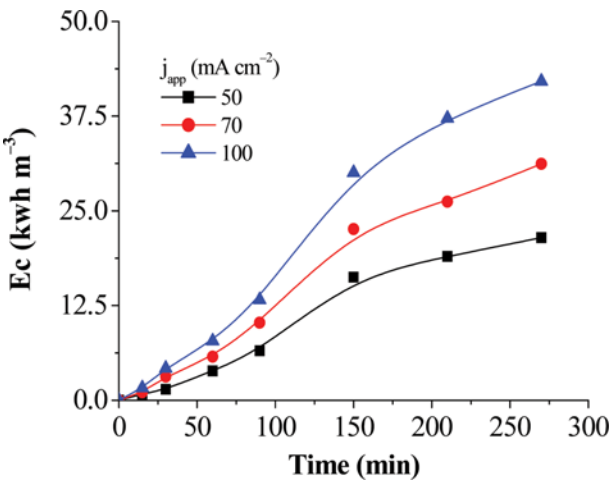

Fig. 9. Evolution of the energy consumption during the electrolysis of IMD (COD(0)=953 mg L^{-1}) on the BDD anode for different applied current densities. Electrolyte: Na_2SO_4 2 g L^{-1}, pH= 3.0 and T=25 °C.

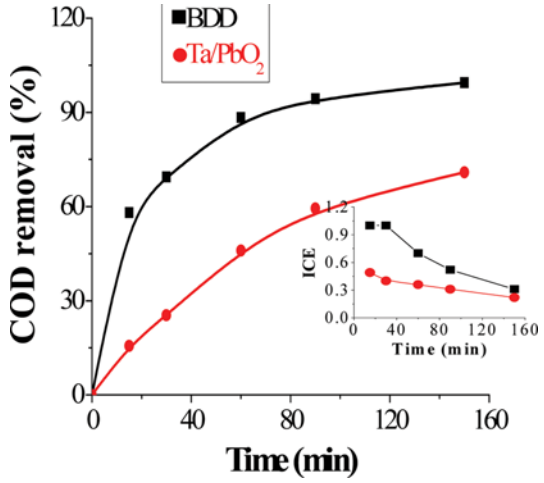

Fig. 10. Comparison of the trend of COD removal and ICE during the electrochemical oxidation of IMD (COD(0)=953 mg L^{-1}) on the BDD and Ta/PbO_2 anodes. Electrolyte: Na_2SO_4 2 g L^{-1}; j_{app}=100 mA cm^{-2}, pH=3.0 and T=65 °C.

obtained at the Ta/PbO_2 anode. This result can be related to the adsorption properties of these two materials. Bearing in mind that the BDD anode has low adsorption properties [30], the hydroxyl radicals generated at the BDD anode were very weakly adsorbed, and consequently more active and effective because they react very rapidly with the organic species arriving at the surface of the anode. However, the PbO_2 anode does not have a higher oxidation state. Consequently, it is classified as a nonactive electrode. It was reported that lead dioxide electrode is a hydrated one, and the electrogenerated hydroxyl radicals are expected to be more strongly adsorbed on its surface and, therefore, less reactive. Today, the PbO_2 is a commercially available material, while BDD, not yet accessible at large scale, can be a good candidate for electrochemical treatment of waste waters polluted by organics.

CONCLUSION

Electrochemical oxidation has proven to be an efficient technology that is suitable for the treatment of wastewater. The advantage of anodic oxidation reactions makes electrochemical oxidation an interesting treatment option for wastewater. The choice of the anode material is crucial, as the specific interaction between the anode surface and the compounds in solution orients the degradation routes of these compounds. We studied the electrochemical removal of IMD on different electrode materials such as the Ta/PbO_2 and BDD anodes using anodic oxidation process. By using both electrodes, the electrochemical degradation of IMD was successfully accomplished. The degradation efficiency at BDD anode increased by increasing the current density and temperature, but it decreased by increasing the initial chemical oxygen demand and the initial pH. Under our experimental conditions, the oxidation was under mass transport control and the COD removal was well described by a pseudo-first-order kinetic. For comparison purposes, the degradation of IMD on BDD anode provided an oxidation rate and current efficiency higher than Ta/PbO_2 for the same operating conditions. This preliminary study suggests that anodic oxidation with BDD electrode constitutes a viable method for the treatment of effluents contaminated by IMD and related pesticides.

ACKNOWLEDGEMENT

This work was financially supported by the Tunisian Ministry of Higher Education and Scientific Research.

REFERENCES

1. L. C. Shirley and E. C. John, *Pestic. Biochem. Physiol.*, **58**, 77 (1997).
2. J. W. Mullins, *Am. Chem. Soc. Symp. Ser.*, **524**, 183 (1993).
3. U. Kapoor, M. K. Srivastava, A. K. Srivastava, D. K. Patel, V. Garg and L. P. Srivastava, *Environ. Toxicol. Chem.*, **32**, 723 (2013).
4. J. K. Lee, K. C. Ahn, O. S. Park, S. Y. Kang and B. D. Hammock, *J. Agric. Food. Chem.*, **49**, 2159 (2001).
5. A. Daraghmeh, A. Shraim, S. Abulhaj, R. Sansour and J. C. Ng, *Environ. Geochem. Health*, **29**, 45 (2007).
6. M. Spiteller and A. G. Bayer, Institute for Metabolism Research, Leverkusen-Bayerwerk, Germany, Report No. PF 3950 (2000).
7. R. Zabar, T. Komel, J. Fabjan, M. B. Kralj and P. Trebse, *Chemosphere*, **89**, 293 (2012).
8. V. Kitsiou, N. Filippidis, D. Mantzavinos and I. Poulios, *Appl. Catal. B-Environ.*, **86**, 27 (2009).
9. A. Chatzitakis, E. Nikolakaki, S. Sotiropoulos and I. Poulios, *Catal. Today*, **209**, 60 (2013).
10. N. Philippidis, S. Sotiropoulos, A. Efstathiou and I. Poulios, *J. Photochem. Photobiol. A Chem.*, **204**, 129 (2009).
11. C. A. Zaror, C. Segura, H. Mansilla, M. A. Mondaca and P. Gonzalez, *Water Practice Technol.*, **4**, 10 (2009).
12. C. Segura, C. Zaror, H. D. Mansilla and M. A. Mondaca, *J. Hazard. Mater.*, **150**, 679 (2008).
13. S. Sharma, B. Singh and V. K. Gupta, B*ull. Environ. Contam. Toxicol.*, **93**, 637 (2014).
14. J. C. Anhalt, T. B. Moorman and W. C. Koskinen, *J. Environ. Sci. Health B*, **42**, 509 (2007).
15. M. Bourgin, J. Albet and F. Violleau, *J. Environ. Chem. Eng.*, **1**, 1004 (2013).
16. M. Bourgin, F. Violleau, L. Debrauwer and J. Albet, *J. Hazard. Mater.*, **190**, 60 (2011).
17. R. M. A. Q. Jamhour, *Can. Chem. Trans.*, **2**, 535 (2014).
18. M. Zahoor and M. Mahramanlioglu, *Chem. Biochem. Eng. Q.*, **25**, 55 (2011).
19. K. Juttner, U. Galla and H. Schmieder, *Electrochim. Acta*, **45**, 2575 (2000).
20. D. Kim, Y. Song and Y. Park, *Korean J. Chem. Eng.*, **30**, 664 (2013).
21. P. Garrett, *Int. J. Agr. Env.*, **1**, 53 (2013).
22. S. A. Abdel-Gawad, K. A. Omran, M. M. Mokhatar and A. M. Baraka, *J. Am. Sci.*, **7**, 134 (2011).
23. S. A. Abdel-Gawad, A. M. Baraka, K. A. Omran and M. M. Mokhtar, *Int. J. Electrochem. Sci.*, **7**, 6654 (2012).
24. M. Turabik, N. Oturan, B. Gozmen and M. A. Oturan, *Environ. Sci. Pollut. Res. Int.*, **21**, 8387 (2014).
25. O. Iglesias, J. Gomez, M. Pazos and M. S. Angeles, *Appl. Catal. B-Environ.*, **144**, 416 (2014).

26. Y. Wang, H. Zhao, S. Chai, Y. Wang, G. Zhao and D. Li, *Chem. Eng. J.*, **223**, 524 (2013).
27. H. Zhao, Y. Wang, T. Cao and G. Zhao, *Appl. Catal. B-Environ.*, **125**, 120 (2012).
28. M. Hupert, A. Muck, R. Wang, J. Stotter, Z. Cvackova, S. Haymond, Y. Show and G. M. Swain, *Diam. Relat. Mater.*, **12**, 1940 (2003).
29. G. R. Salazar-Banda, L. S. Andrade, P. A. P. Nascente, P. S. Pizani, R. C. Rocha-Filho and L. A. Avaca, *Electrochim. Acta*, **51**, 4612 (2006).
30. H. B. Suffredini, V. A. Pedrosa, L. Codognoto, S. A. S. Machado, R. C. Rocha-Filho and L. A. Avaca, *Electrochim. Acta*, **49**, 4021 (2014).
31. M. Errami, R. Salghi, A. Zarrouk, A. Chaki, S. S. Al-Deyab, B. Hammouti, L. Bazzi and H. Zarrok, *Int. J. Electrochem. Sci.*, **7**, 4272 (2012).
32. C. Te-San, T. Ren-Wei, C. Yu-Syuan and H. Kuo-Lin, *Int. J. Electrochem. Sci.*, **9**, 8422 (2014).
33. H. Bouya, M. Errami, R. Salghi, B. Gozmen and M. Messali, *J. Mater. Environ. Sci.*, **35**, 1565 (2014).
34. A. S. Alves, C. R. T. Ferreira, L. F. L. Migliorini, R. M. Baldan, G. N. Ferreira and R. V. M. Lanza, *J. Electroanal. Chem.*, **702**, 1 (2013).
35. A. M. Trautmann, H. Schell, K. R. Schmidt, K. M. Mangold and A. Tiehm, *Water Sci. Technol.*, **71**, 1569 (2015).
36. F. Cardarelli, P. Taxil and A. Savall, *Int. J. Refract. Met. Hard. Mater.*, **14**, 365 (1996).
37. M. Pourbaix, Atlas d'Equilibres Electrochimiques à 25 °C, Gauthier-Villars, Paris (1963).
38. A. Perret, W. Haenni, N. Skinner, X. N. Tang, D. Gandini, C. Comninellis, B. Correa and G. Foti, *Diam. Relat. Mater.*, **8**, 820 (1999).
39. I. M. Kolthof, E. B. Sandell, E. J. Meehan and S. Buckstein, *Quantitative chemical analysis*, 4th Ed., Macmillan, New York, 1862 (1969).
40. C. Comninellis and C. Pulgarin, *J. Appl. Electrochem.*, **21**, 703 (1991).
41. E. Hmani, S. E. Chaabane, Y. Samet and R. Abdelhédi, *J. Hazard. Mater.*, **170**, 928 (2009).
42. Y. Samet, L. Agengui and R. Abdelhédi, *J. Electroanal. Chem.*, **650**, 152 (2010).
43. S. Kongjao, S. Damronglerd and M. Hunsom, *Korean J. Chem. Eng.*, **25**, 703 (2008).
44. O. J. Murphy, G. D. Hitchens, L. Kaba and C. E. Verostko, *Water Res.*, **26**, 443 (1992).
45. Z. Wu, Y. Cong, M. Zhou, Q. Ye and T. Tan, *Korean J. Chem. Eng.*, **19**, 866 (2002).
46. M. Panizza, P. A. Michaud, G. Cerisola and C. Comninellis, *J. Electroanal. Chem.*, **507**, 206 (2001).
47. E. Petrucci and D. Montanaro, *Chem. Eng. J.*, **174**, 612 (2011).
48. P. Canizares, E. Mahe, W. Haenni, A. Perret and C. Comninellis, *Electrochem. Solid-State Lett.*, **3**, 77 (2000).
49. J. Rodriguez, M. A. Rodrigo, M. Panizza and G. Cerisola, *J. Appl. Electrochem.*, **39**, 2285 (2009).
50. N. Belhadj-Tahar and A. Savall, *J. Electrochem. Soc.*, **145**, 3427 (1998).
51. N. Rabaaoui, Y. Moussaoui, M. S. Allagui, B. Ahmed and E. Elaloui, *Sep. Purif. Technol.*, **107**, 318 (2013).
52. O. Dridi Gargouri, Y. Samet and R. Abdelhedi, *Water SA*, **39**, 31 (2013).
53. O. ID El Mouden, M. Errami, R. Salghi, A. Zarrouk, M. Assouag, H. Zarrok, S. S. Al-Deyab and B. Hammouti, *J. Chem. Pharm. Res.*, **4**, 3437 (2012).
54. E. Weiss, K. G. Serrano and A. Savall, *J. Appl. Electrochem.*, **38**, 329 (2008).
55. A. Serra, X. Domenech, J. Peral, C. Arias and E. Brillas, *J. Environ. Eng. Manage.*, **18**, 173 (2008).